Cite this article
Brown MJ, Davidson C, Shepherd CJ, Flint SM and Mbisike S (2026)
Sustainable overhead line equipment foundations with optimised shape and backfilling.
Proceedings of the Institution of Civil Engineers – Geotechnical Engineering **179(2)**: 173–186,
https://doi.org/10.1680/jgeen.25.00151

Research Article
Paper 2500151
Received 19/07/2025; Accepted 18/11/2025

Geotechnical Engineering

Sustainable overhead line equipment foundations with optimised shape and backfilling

Michael John Brown
School of Science and Engineering, University of Dundee, Dundee, UK
(Orcid:0000-0001-6770-4836) (corresponding author:
m.j.z.brown@dundee.ac.uk)

Craig Davidson
School of Science and Engineering, University of Dundee, Dundee, UK
(Orcid:0000-0002-4843-5498)

Charlie John Shepherd
School of Science and Engineering, University of Dundee, Dundee, UK
(Orcid:0000-0003-0607-592X)

Stuart Martin Flint
Scottish and Southern Electricity Networks (SSEN), Glasgow, UK

Stephen Mbisike
National Grid Electricity Transmission (NGET), Warwick, UK
(Orcid:0000-0003-0013-4829)

Methods to enhance the tensile capacity and optimise the design of concrete pad foundations for overhead line equipment were investigated with the aim of reducing environmental impacts and costs. Using finite-element analysis and centrifuge modelling in sand, the effects of chamfering the pad's upper edge and varying the density of the material used to backfill the excavation were explored. A 30–40° chamfered edge on the pad increased the tensile capacity by up to 40% at low embedment ratios, shifting the failure surface origin from the pad top to the bottom. The backfill density above the foundation was shown to influence the failure mechanisms. When the backfill was less dense than the native soil, vertical failure surfaces formed. Conversely, when the relative densities of both the backfill and native soil were 60% or higher, transitional shear planes emerged. When the backfill's relative density exceeded that of the native soil, an increase in uplift capacity was observed. However, the effectiveness of backfilling appears to be sensitive to disturbance at the vertical excavation interface. Sloping the backfill sides to 25° allowed the failure surface to develop at the soil's dilation angle, independent of excavation effects. These findings offer practical strategies to improve foundation efficiency and sustainability in overhead line projects.

Keywords: centrifuge modelling/electrical engineering & distribution/finite-element modelling/foundations/geotechnical engineering/model tests/shallow foundations

Notation

A	foundation base area
B	foundation width/breadth
D_{10}	effective particle size
D_{50}	average particle size
D_r	relative density
d	vertical uplift displacement
E_{50}	secant triaxial stiffness
E_{oed}	oedometer loading stiffness
E_{ur}	triaxial unloading stiffness
G_0	maximal small-strain shear modulus
H	depth to failure surface origin
N	centrifuge scaling factor
N_γ	breakout factor
Q_u	total uplift capacity
R_{in}	interface reduction factor
α	pad chamfer angle
γ	soil unit weight
ε_1	principal strain in finite-element (FE) modelling
ϕ_{cs}	critical state friction angle

1. Introduction

In the UK there is currently significant effort being made to upgrade the electrical transmission infrastructure to meet the ever-increasing demand for electricity and to allow transmission from new remote areas of renewable energy generation such as onshore and offshore windfarm projects (DBEIS, 2022). It is currently estimated that there are 90 000 overhead line equipment (OLE) towers in the UK, and this is predicted to double. It has been estimated that a spend of £58 billion is required between 2030 and 2035, on top of the current investment to 2030 of £54 billion (BBC, 2024). With all this planned and ongoing construction, it is important that this initiative is not only used to enhance new structures but also to increase efficiency and reduce the carbon dioxide footprint and environmental impacts.

A significant component of new OLE construction is the foundation system, with these often consisting of reinforced concrete buried pad and column type structures (Gu *et al*., 2024). With four of these typically one at each lower corner of a lattice OLE tower structure, there is much associated construction effort through excavation, excavation support, reinforcement tying, concreting and backfilling. These are the obvious operations but, depending on the location of the OLE towers, they can be at significant distances from existing road networks and in potentially mountainous regions (e.g. upland Scotland). This then requires the construction of new heavily rated haul roads through potentially sensitive

environments and peat bogs, which further increases the carbon dioxide impact. Multiply this by four and then 90 000, and the potential resource use and impact becomes obvious.

With a view to improving the efficiency of such foundations under the most critical load path (tension or uplift) (BSI, 2013a; Kulhawy *et al*., 1983; Vanner, 2003), a series of investigations have been undertaken looking at potential efficiency enhancements initially focused on improved design techniques (Brown *et al*., 2025). Other identified potential enhancements include modification of foundation shape to reduce foundation volume and concrete material, and optimising backfilling densities and the shape of the backfilled zone above the foundation. The latter study, based on comments made and summarised by Levy (2014), showed that the full extent of an inclined excavation is not mobilised unless the backfill is of similar soil type or compacted to equivalent density and stiffness. It has also been reported that backfill compaction can improve uplift capacity by up to 4.5 times (Zmudzinski and Sala, 1980). Other potential alternatives such as returning to concrete-less grillage foundation options are also being explored (Shepherd *et al*., 2024).

Investigation into changes in shape seems logical as this has the potential to easily reduce concrete volumes. However, it is also useful to explore the evolution of the shape/type of OLE foundation used in the UK, where historically these were steep pyramids, with a pad chamfer angle (α) of 20–45° (Figure 1(b)). Although examples of shallow pyramids ($\alpha = 65°$) exist in the literature (Cigre, 2002), nowadays it is much more common to adopt a pad and column type structure, but a modified pad foundation has the potential for reduced volume and only slightly less capacity than the pad and column type (Brown *et al*., 2025). The evolution of the shape and form of OLE foundations is not particularly clear except as stated above, where it would appear the transition from pyramidal shape has been driven more by practical concerns and modern construction practices rather than optimisation of uplift capacity (Vanner, 2003).

The development of more realistic foundation and excavation approaches for centrifuge application (Brown *et al*., 2025) allow the study of backfilling at different densities at appropriate stress levels. Previous studies based on 1***g*** modelling exist, but the effects of low-stress regimes in the modelling of different backfilling regimes and resulting mechanisms have not previously been explored. It is also the case in some previous small-scale models that the excavation was unsupported during formation and backfilling (Kulhawy *et al*., 1991) and does not reflect current UK construction processes. That said, Kulhawy *et al*. (1991) developed a framework for characterising backfill behaviour and its influence on uplift capacity, which varied with depth and the backfill to native soil density ratio. They also attempted to inspect the failure mechanism to see how these different variables controlled mechanisms by post-test excavation of their 1***g*** models. Current guidance (e.g. BSI, 2013b) suggests that backfill compaction should be undertaken to achieve soil characteristics as close as possible to the native undisturbed soil, but does not suggest if this can be optimised or not. This guidance also seems to align more with approaches to design (i.e. the selection of consistent design input densities and shear strengths (BSI, 2013a: annex M) based upon in situ pre-construction investigation rather than an attempt to optimise behaviour. Kulhawy *et al*. (1991) suggested achieving in situ conditions may be challenging in the field and that backfill density would alter the prevailing failure mechanisms. Apart from the research undertaken by Kulhawy *et al*. (1991), there seems to be a dearth of information on backfilling optimisation or centrifuge studies in granular material in the academic literature. Most studies are concerned with behaviour in uniform soils with a more fundamental focus, and do not consider wider practical concerns (Gu *et al*., 2024). That said, alternative backfilling options in clay parent material such as loose sand, cement-improved clays and

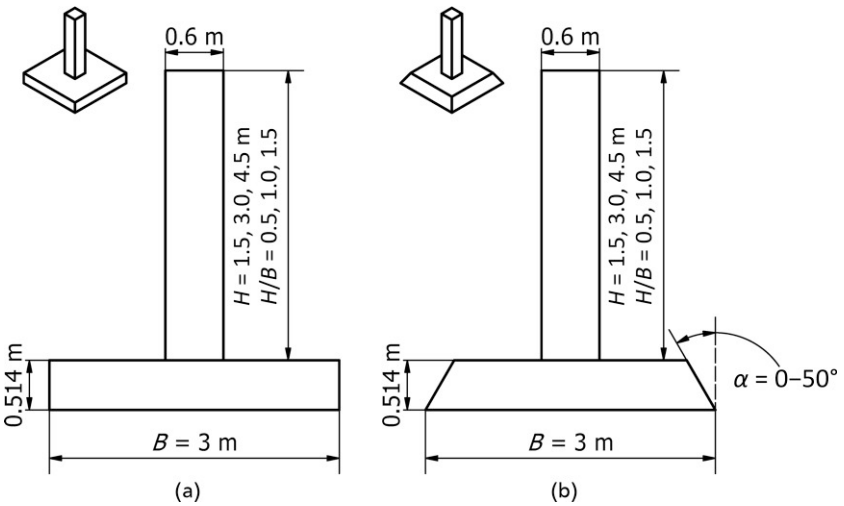

Figure 1. Prototype-scale foundation geometries: (a) pad; (b) optimised pad

type 2 DOT have previously received attention (Rattley *et al*., 2008; Richards *et al*., 2010; Levy, 2014).

This paper summarises an investigation using finite-element analysis (FEA) and appropriately scaled centrifuge testing at prototype stress levels to look at two potential methodologies to improve OLE foundation performance, including altering the geometry of existing pad and column foundations with a view to reducing concrete material volumes. This was followed by a backfilling investigation, which looked at varying backfilling densities relative to the native soil and also changing the excavation shape to optimise construction approaches. The aim of the latter was to investigate historical field studies that suggest failure occurs in the backfill rather than on an inclined excavation surface (Parr and Vanner, 1962; Vanner, 2003). Centrifuge testing was adopted to overcome the scaling issues associated with previous 1***g*** studies. Physical model testing was also designed to incorporate more realistic foundation installation techniques, as introduced by Brown *et al*. (2025).

2. Methodology

2.1 FEA

Initially, three-dimensional (3D) finite-element (FE) studies were performed to investigate the influence of the foundation depth, soil properties, foundation shape and the effect of backfilling at different densities and in differently shaped excavations. For the study of foundation shape, the soil was modelled in a uniform manner. For backfilling studies, the backfill–native soil interface was also considered using interface elements, as explained later in this section.

The geometry of the foundation was that of a pad and column (or chimney) (Figure 1(a)), which was then modified in the shape optimisation study (Figure 1(b)). To investigate embedment depth effects, the foundation geometry was kept constant and the length of the column was adjusted. In all cases, to simplify the analysis, the column was modelled vertically aligned rather than inclined (typically 10–15° in the field) as this was previously shown to have little effect on the results (Brown *et al*., 2025). Details of the foundation geometries are presented in Figure 1. These reflect typical current geometries adopted in the UK for a pad and column foundation (Figure 1(a)) (based on information supplied by Scottish and Southern Electricity Networks and National Grid Electricity Transmission). Figure 1 also provides definitions of the foundation embedment depth (H) and width (B) used to determine the embedment ratio (H/B).

Plaxis 3D (version 2023.2) was used for the 3D FEA. This software uses constitutive models to define the behaviour of the FE mesh, which represents the soil. The hardening soil with small strain (HS small) constitutive model (Bentley Systems, 2017) was used with parameters for HST95 sand (Table 1) routinely used for physical modelling at the University of Dundee (Al-Defae, 2013; Al-Defae *et al*., 2013; Bertalot, 2013; Bertalot *et al*., 2013; Lauder, 2010; Lauder *et al*., 2013). The HS small model uses effective stress parameters to define the limiting stress of the soil by using the peak friction angle, dilation angle and cohesion as per Mohr–Coulomb models. However, the stiffness of this advanced constitutive model is based upon three distinct stiffness parameters – triaxial stiffness (E_{50}), triaxial unloading stiffness (E_{ur}) and oedometer loading stiffness (E_{oed}) – at a reference stress of 100 kPa. The stiffness at small strain is also included in the HS small model to provide improved accuracy in modelling the non-linear elastic strain.

To investigate the influence of the foundation shape, the pad was modified by adding a chamfer of varying angle (α) at the upper edge of the pad, as shown in Figure 1(b). The resulting reductions in concrete volume are shown in Table 2. Analysis of the foundation in uniform sand was completed to model the foundation in relative densities (D_r) of 30%, 60% and 90% and embedment depths of depths (H) to the base of the foundation of ∼2, 3 and 5 m ($H/B = 0.5$, 1.0 and 1.5 at the pad top, where B is the width of the foundation (3 m in this study)). Drained conditions were assumed for all sand models and dry unit weights were employed

Table 1. Properties of HST95 sand used in FEA (Al-Defae *et al*., 2013; Al-Defae, 2013)

Property	$D_r = 30\%$	$D_r = 60\%$	$D_r = 90\%$
Dry unit weight, γ: kN/m^3	15.4	16.3	17.2
Peak friction angle, ϕ_{pk}: degrees	35	41	47
Dilation angle, ψ: degrees	3.4	11.2	19
Critical state friction angle, ϕ_{cs}: degrees	32	32	32
Interface friction angle with cast concrete, δ: degrees ($2/3\phi_{cs}$ (BSI, 2013a))	21.3	21.3	21.3
Secant modulus, E_{50}: kN/m^2	34 650	44 025	53 400
Tangent oedometric modulus, E_{oed}: kN/m^2	27 720	35 220	42 720
Unloading–reloading stiffness, E_{ur}: kN/m^2	83 100	105 600	128 100
Stiffness exponent for minor stress formulation, m	0.57	0.54	0.51
Maximal small-strain shear modulus, G_0: kN/m^2	103 800	118 800	133 800
Value of small strain for which G_s/G_0 reduces to 0.722, $\gamma_{0.7}$: kN/m^2	0.0001180	0.0001690	0.0002200
Failure ratio, R_f	0.9	0.9	0.9
Cohesion intercept, c: kN/m^2	0.2	0.2	0.2
At-rest earth pressure coefficient, K_0	0.426	0.344	0.269

Table 2. Reduction in concrete volume of chamfered pads (3 m wide, 3 m deep, 0.514 m thick)

Chamfer angle, α: degrees	Volume: m^3	Volume difference compared with 0° chamfer: %
0	4.63	—
10	4.35	6
20	4.07	12
30	3.77	18
40	3.42	26
50	2.99	35

throughout. An example of the generated FE mesh is shown in Figure 2, which illustrates the mesh refinement employed around the foundation to improve accuracy. Fine to medium meshing algorithms were used with 15-point triangular elements, resulting in approximately 105 000 total elements in the model. The foundation was modelled as a rigid body, which avoided using alternative element types with very large stiffnesses that can create errors in the stiffness matrix. The boundary conditions of the rigid body were set to prevent horizontal translation or rotation, allowing vertical movement only. Boundary conditions/positions of the model were checked with a mesh optimisation study to ensure there was no influence from the side or base boundary. Loading of the foundation was achieved by displacement-controlled movement of the rigid-body foundation (as a single object) by a total of 30 mm vertically upwards. The self-weight of the above-ground OLE structure was not considered during this study. Zero-thickness interface elements were included at the foundation element boundaries to allow for the inclusion of a strength reduction factor to account for the soil–structure interface friction. The interface friction of sand on a cast concrete surface is widely modelled as $2/3\phi_{cs}$ (BSI, 2013b) and this value was adopted for all the sand models. This was implemented in Plaxis by modifying its interface reduction factor (R_{in}) for the three soil densities to maintain a constant value for the interface friction angle as per Table 1.

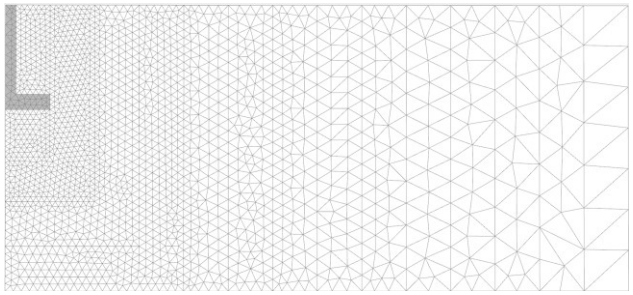

Figure 2. Example of FE mesh showing a higher degree of mesh refinement close to the foundation

In terms of modelling the backfill, two arrangements were explored.

- Firstly, with the backfill vertically inclined (as shown in Figure 3(a)) to mimic UK construction.
- Secondly, to investigate the potential constraint of a vertically supported backfill, inclined excavation simulations were also undertaken with sides battered back at 25° to check if current practice is constraining capacity (Figure 3(b)).

The backfilled soil was created at relative densities of 30%, 60% and 90% down to the depth of the foundations. Only normally consolidated conditions were modelled (i.e. stress increases from compaction were not considered). However, in reality, such increases may be negated by the removal of sheet piles during the construction process. To simulate the backfilling process in the FEA, interface elements were included with $R_{in} = 1$ to ensure a rigid (fully rough) soil–soil interface and with R_{in} modified to give a disturbed interface and set to return the critical state friction angle of the HST95 sand ($\phi_{cs} = 32°$). These two extremes of interface then allowed exploration of the potential effects of backfill–native soil interface construction on the results. These interfaces were either inclined vertically or at 25°, as shown in Figure 3. Where the backfilling process was compared with uniform soil, no interface elements were included (see Section 3.2).

Both types of modelling were compared with centrifuge testing to give confidence in the findings. The programme of FE simulations is summarised in Tables 3 and 4.

2.2 Centrifuge physical modelling

The University of Dundee's 3 m Actidyn centrifuge was used for all testing with a scaling factor of 42.85. This maintained the same

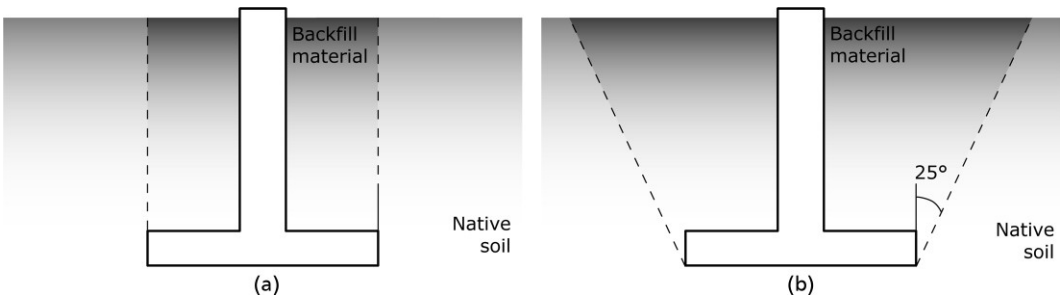

Figure 3. Foundation and backfilled material configurations: (a) vertical backfill; (b) 25° sloped backfill

Table 3. Summary of FE simulations for backfill investigation

Native sand relative density: %	Backfill relative density: %	Backfill side angle: degrees
30 (uniform conditions)	No backfill	—
60 (uniform conditions)	No backfill	—
90 (uniform conditions)	No backfill	—
30	30, 60, 90	0
60	30, 60, 90	0
90	30, 60, 90	0
30	30, 60, 90	25
60	30, 60, 90	25
90	30, 60, 90	25

Table 4. Summary of FE simulations for shape optmisation study. All permutations of depth and relative density were simulated for each chamfer angle (total of 54 simulations)

Embedment ratio, H/B	Relative density, D_r: %	Chamfer angle, α: degrees
0.5, 1.0, 1.5	30, 60, 90	0
		10
		20
		30
		40
		50

key dimensions to be consistent with the numerical modelling (e.g. $B = 3$ m) as per Figure 1. All the model length and displacements were scaled by N and the weight/force by N^2. Vertical uplift (2 mm/min model scale) of the model foundation was achieved with displacement-controlled movement of an actuator developed at the University of Dundee (Al-Baghdadi *et al*., 2016; Davidson *et al*., 2018). The actuator was manually moved laterally along the 800 × 500 mm model container between tests to enable two tests in each box. Uplift forces were continuously measured by a 20 kN F310-Z instrument (Novatech Measurements Ltd). The connection between the model and actuator allowed the foundation to settle during ***g***-up of the centrifuge before with the gap being closed up on starting the loading event. Vertical foundation displacement was measured by a WDS-750-P60-CR-P draw-wire transducer. Additional details on the control and logging system are available elsewhere (Brown *et al*., 2025).

The model foundations were 1:42.85 scale models (N) of pad and column foundation, as shown in Figure 1. The base and columns of the models were typically fabricated from 6061 aluminium. The aluminium used in the centrifuge tests was chosen to be significantly stiffer than reinforced concrete so that soil stiffness/failure alone could be considered in isolation. This is in line with the numerical modelling, where the foundations were modelled as rigid objects. However, for studying the variation in pad geometry, the non-standard foundations were formed from 3D printed acrylonitrile butadiene styrene (ABS) plastic to allow rapid prototyping. To check for any stiffness variations between the two foundation materials, two chamfered foundations were also created in 6061 aluminium with no noticeable differences between the load–displacement results from the two foundation materials. In all cases, the base of the foundation was manufactured separately to the column portion for easy alteration of the embedment depth by using different length columns. An M8 countersunk socket head screw was used to connect the pad and column together. No additional surface interface preparation was undertaken for the foundation models as FE modelling of rough and smooth interfaces showed little effect on the results because failure tended to occur in the soil body. As the FE model assumed weightless foundations, the weight of the foundations was subtracted from the measured loads. Dry HST95 sand was used in all centrifuge modelling to avoid any potential influence of suction and rate effects during uplift. HST95 is a fine sand with $D_{10} = 0.10$ mm and $D_{50} = 0.14$ mm (Lauder *et al*., 2013). Relevant properties of the HST95 sand are provided in Table 5. All the soil beds were created by means of dry air pluviation (Ueno, 1998). Details of the sand bed preparation are provided by Brown *et al*. (2025) and the centrifuge testing programme is summarised in Tables 6 and 7. This also includes the process for excavation support and backfilling in the case of the vertical backfill tests. Tests on different foundation shapes were undertaken in uniformly pluviated sand beds only and backfilling was not simulated.

3. Results and discussion

3.1 Shape optimisation

The baseline case for the shape optimisation study was the pad and column foundation with a zero-chamfer angle ($\alpha = 0°$), as shown in Figure 1(a). In this case, the depth of the foundation (H) was defined from the soil surface to the top of the foundation. Figure 4 shows the results of the FEA simulation and the evolution of the failure plane position in medium dense sand; for $\alpha = 0°$, the failure plane clearly emanated from the top corner of the foundation inclined at the dilation angle. With an increase in the chamfer angle between 20° and 40°, the failure surface bifurcated and a second failure surface developed from the bottom of the chamfered edge at the base of the foundation. At $\alpha = 40°$, the failure surface originating at the base of the chamfer/foundation was dominant. This led to an effective gain of 0.514 m depth of embedment for this foundation arrangement.

Table 5. Properties of HST95 sand from centrifuge tests (Al-Defae, 2013; Lauder, 2010)

Property	Value
Effective particle size, D_{10}: mm	0.09
Average particle size, D_{50}: mm	0.14
Critical state friction angle, ϕ'_{crit}: degrees	32
Angle of dilation[a] at $D_r = 60\%$, ψ: degrees	11.2
Peak friction angle[a] at $D_r = 60\%$, ϕ'_{pk}: degrees	41
Maximum dry density, ρ_{max}: kN/m^3	17.58
Minimum dry density, ρ_{min}: kN/m^3	14.59

[a]Inferred from best-fit peak strength relationship from direct shear tests for data at effective stresses between 50–200 kPa and critical state friction angle, at $D_r = 60\%$ (Al-Defae *et al*., 2013)

Table 6. Summary of centrifuge tests for shape optimisation study of pad foundation

Test	Relative density, D_r: %	Embedment ratio, H/B	Chamfer angle, α: degrees	Model material
C1	61	1.0	0	ABS
C2	61	1.0	10	ABS
C3	60	1.0	20	ABS
C4	60	1.0	30	ABS
C5	60	1.0	40	ABS
C6	60	1.0	50	ABS
C7	44	0.5	30	Aluminium
C8	44	1.0	30	Aluminium
C9	44	1.5	30	Aluminium
C10	60	0.5	30	Aluminium
C12	60	1.0	30	Aluminium
C13	60	1.5	30	Aluminium

Table 7. Summary of centrifuge tests for backfill investigation of pad foundation

Test	Embedment ratio, H/B	Relative density of native sand: %	Relative density of vertical backfill: %
B1	1.0	60	60
B2	1.0	60	83

The results of varying the chamfer angle on uplift capacity for different variables (e.g. sand density and normalised embedment depth) are shown in Figure 5. Figure 6–8 show that the effect of increasing the chamfer angle appeared to be most noticeable at $H/B = 0.5$ and reduced with increasing depth (Figures 7 and 8). That said, there was still a significant increase in capacity at $H/B = 1.5$ (15%) and up to 40% at $H/B = 0.5$. It is also noticeable that the chamfer angle appeared to reach a certain point (e.g. 30° in dense soil at $H/B = 0.5$), after which there was no further enhancement in behaviour with an increase in chamfer angle. This transition point seemed to change with the soil density, suggesting it is affected by effective stress and soil density, which would suggest that the dilation angle controls this transition point. To capture this behaviour in the various scenarios, a chamfer angle of 30–40° seems to be the best approach. Increasing the chamfer angle above this would not give additional capacity benefits but would still save concrete volume (Table 2).

To verify the results, similar simulations were undertaken in centrifuge tests (Table 6). Figure 9 shows the load–displacement results in loose sand at a $H/B = 1.0$ for the complete pull-out event to 200 mm at prototype scale, which significantly exceeded the normal ultimate capacity determination point determined at 25 mm uplift (National Grid TS 3.4.15, 2018). A similar trend of increasing capacity with increasing chamfer angle is clear. Figure 10 shows that the centrifuge test results were comparable with the FEA, although the determination of peak ultimate capacity slightly exceeding the FEA and the determination at 25 mm underpredicting the FEA. While there is some more variability in the trend of the normalised values of the uplift capacity at 25 mm in the centrifuge data, the overall behaviour was broadly similar to the FEA results. The scatter may be a result of variation in the stiffness response of the foundation to tensile load and also probably reflects some elements of realistic sample formation.

3.2 Backfilling density

The implementation of a more realistic backfilling model formation sequence conducted by Brown *et al*. (2025) showed that backfilling has the potential to modify foundation behaviour during uplift and promote failure along a vertically inclined failure plane, even when the excavation support is removed. Implementing this improvement in the physical modelling allowed the backfilling process to be investigated for different backfilling densities but, prior to this, the decision was made to perform an initial FEA study to gauge its potential to model the effect and allow a greater set of parameters to be explored.

Initially, backfilling was modelled using FEA with a vertical excavation as previously discussed (Figure 3(a)). The vertical strain after 25 mm vertical upward displacement of the foundation in uniform and backfilled conditions is shown in Figure 11. Results from a previous centrifuge modelling study (Brown *et al*., 2025) showed that even with pluviated backfill at the same relative density as the native soil there was a reduction in ultimate capacity (of 29% for medium dense backfill in medium dense native material, $H/B = 1$), even when the backfill and native soil densities were matched due to disturbance from removal of the excavation support.

The results of FEA with the vertical excavation elements set at $R_{in} = 1$, denoting minimal installation effects, are presented in Figure 11. In all cases, where the vertical backfill soil was modelled at a density notably lower than the surrounding soil, the failure surface created by the uplift of the foundation tended to occur at the interface between the backfill and surrounding soil, as shown in Figure 11. Kulhawy *et al*. (1991) refer to this as a side shear mode. When both the native and backfill soils had relative densities of 60% (1662 kg/m^3) or greater, in any combination (Figures 11(h), 11(i), 11(k) and 11(l)), the FEA seems to show more transitional behaviour with the failure moving from a predominantly vertical situation towards wedge failure. This may

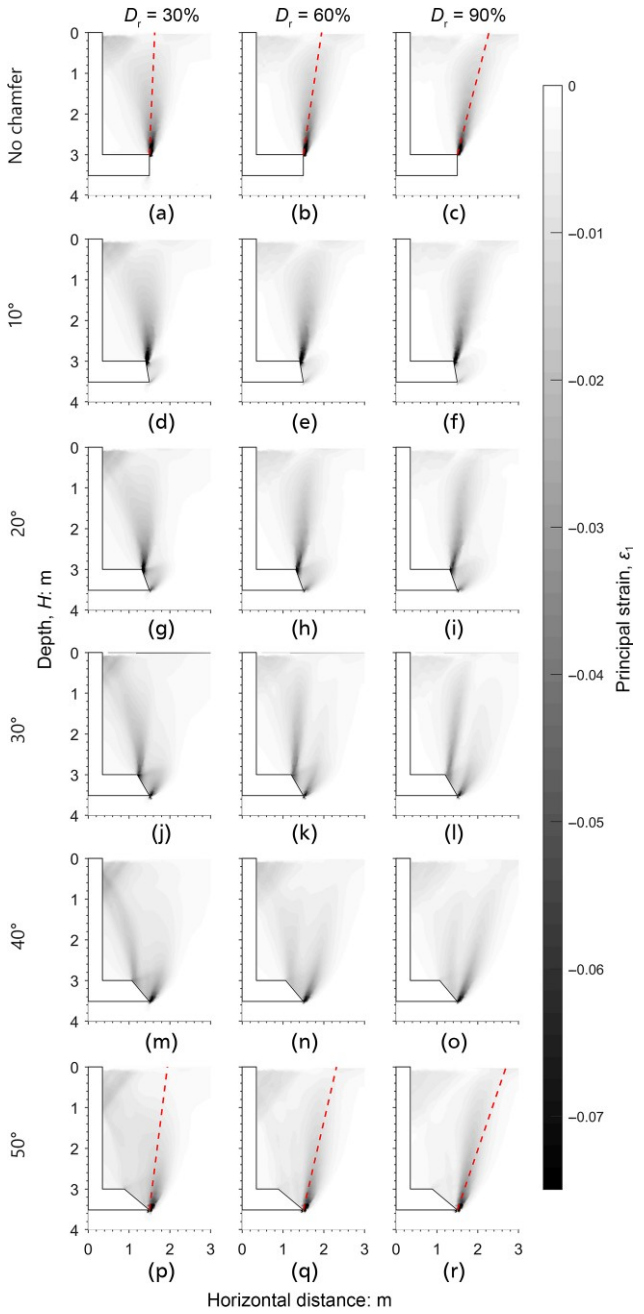

Figure 4. Principal strain after 30 mm uplift of 0–50° chamfered pad at an embedment ratio (*H*/*B*) of 1 (pad top) in sand of increasing relative densities (D_r = 30, 60 & 90% or 1570, 1662 & 1754 kg/m^3). The red dashed lines indicate the dilation angle of sand at the respective relative density

explain the combined failure mode described by Kulhawy *et al*. (1991). This is in contrast to the failure surface in uniform sand, where it followed the dilation angle of the sand (Figures 11(a)–11(c)), or where the relative density of the native soil was 30% (1570 kg/m^3), in which case only a near-vertical failure surface was formed (Figures 11(d), 11(g) and 11(j)).

When the excavation interface behaviour was modified to fully disturbed (Figure 12), the behaviour was simplified for all of the backfilling cases and the behaviour was dominated by failure along the excavation interface. Some limited near-surface curvature of the failure plane appeared for increased relative densities of the backfill and native soil, but the effect appears limited. These results are in line with the results from centrifuge testing with realistic construction sequencing reported by Brown *et al*. (2025).

Examination of the load–displacement data (Figure 13) from the numerical simulations shown in Figure 11 for an undisturbed excavation interface (R_{in} = 1) suggests that the uplift load–displacement response of the foundation scenarios were essentially the same in the cases of wholly uniform native sand when there was a backfilled portion of sand with density matching that of the native sand. This is consistent with the tendency towards wedge or inclined failure surface type behaviour (Figures 11(a), 11(b), 11(c), 11(d), 11(h) and 11(l)) observed by Kulhawy *et al*. (1991). In the case of backfill material with D_r = 30% (1570 kg/m^3), the capacity was reduced by approximately 5.4% and 8.4% when the surrounding soil was D_r = 60% (1662 kg/m^3) or greater (Figures 13(b) and 13(c)). This is because of the predominantly vertical failure mode shown in Figures 11(d)–11(f), suggesting there are some gains to be made through appropriate backfill compaction if an enhanced interface can be created or maintained. The shearing resistance is lower due to the failure surface occurring at the vertical backfill/native soil interface (reduced surface area) instead of at the dilation angle of the sand (11.2° for D_r = 60%, 1662 kg/m^3) and the weight of soil contribution is decreased from that within a wedge-shaped failure surface which forms in uniform relative density compared to that of the rectangular failure shape in the backfilled sand.

When the relative density of the backfilled sand was greater than that of the surrounding soil (e.g. backfill of D_r = 90% (1754 kg/m^3) and native sand at D_r = 60% (1662 kg/m^3)), the uplift capacity can be greater than the uniform or matching D_r scenarios, as shown in Figure 12. This occurs due to the increased unit weight of the backfill sand (see Table 1 for values), an increase in shearing resistance from greater normal stress on the failure plane because of the higher unit weight and vertical stress, and the tendency to transition to a transitional or inclined failure surface. The results suggest that, as a minimum, an attempt should be made to match backfill and native soil densities; there may be marginal gains from compacting backfill to higher than the native soil but the benefit needs to be weighed against the effort. However, in loose uniform sands there is no benefit at ultimate capacity of denser backfill.

In contrast, where the excavation interface is fully disturbed (R_{in} set to give ϕ_{cs} = 32°) the results from all the scenarios effectively returned similar behaviour to that seen for uniform loose sand (Figure13(a)) where the behaviour is only controlled by shearing

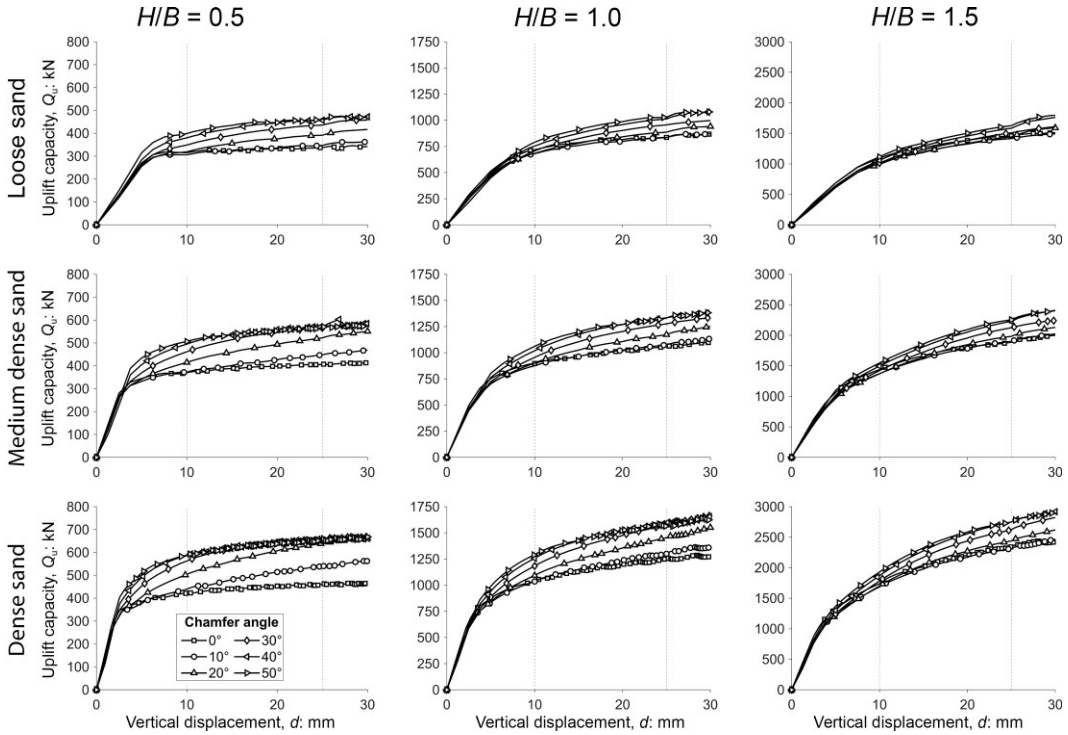

Figure 5. Summary of 3D FEA load–displacement results from uplift of plain and 10–50° chamfered pad foundations with embedment ratios (*H*/*B*) of 0.5, 1.0 and 1.5 in loose, medium dense and dense dry sand

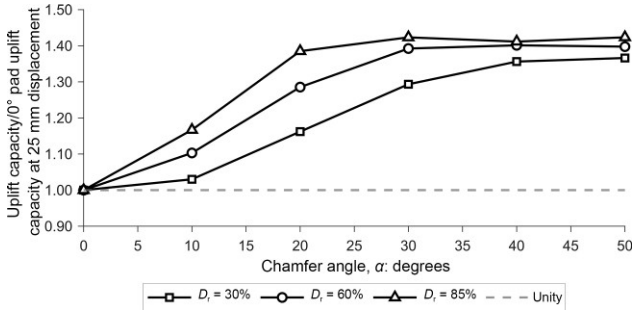

Figure 6. Uplift capacity at 25 mm displacement normalised by capacity of 0° chamfer pad capacity for *H*/*B* = 0.5 in soils of different density

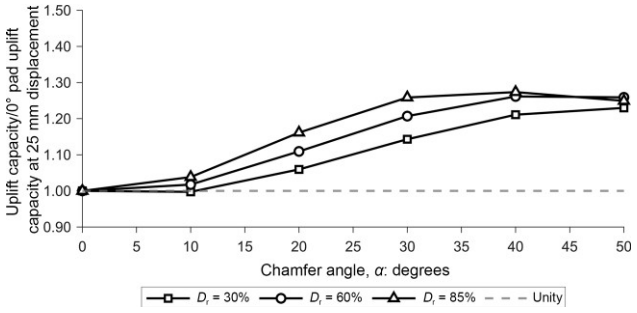

Figure 7. Uplift capacity at 25 mm displacement normalised by capacity of 0° chamfer pad capacity for *H*/*B* = 1.0 in soils of different density

along the interface. With this disturbed interface, the effects of the backfill density become minimal in terms of generating resistance from soil–soil shear and any differences in the uplift capacity with increasing density are a result of the increased mass of soil being uplifted (Figure 13). This suggests the state of the excavation interface is key to maximising any benefits that can be obtained from varying the backfill density and the construction performance achievable.

Comparing the FEA results with the results reported by Kulhawy *et al*. (1991) using a normalised uplift breakout factor showed less obvious improvement (Figure 14). The uplift capacity was compared at 25 mm displacement. The normalised uplift breakout factor was calculated as:

$$N_\gamma = \frac{Q_u}{\gamma A H}$$

where γ is the unit weight of the backfill, Q_u is the uplift force, A is the foundation area and H is the burial depth to the upper surface of the foundation.

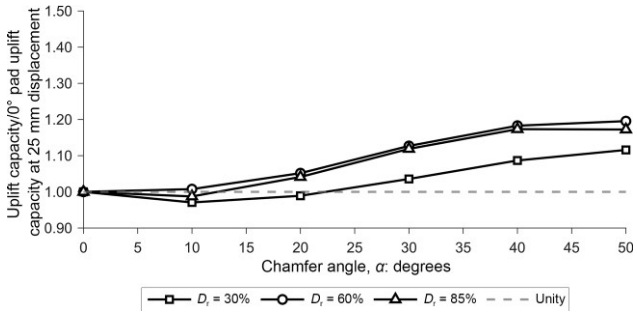

Figure 8. Uplift capacity at 25 mm displacement normalised by capacity of 0° chamfer pad capacity for $H/B = 1.5$ in soils of different density

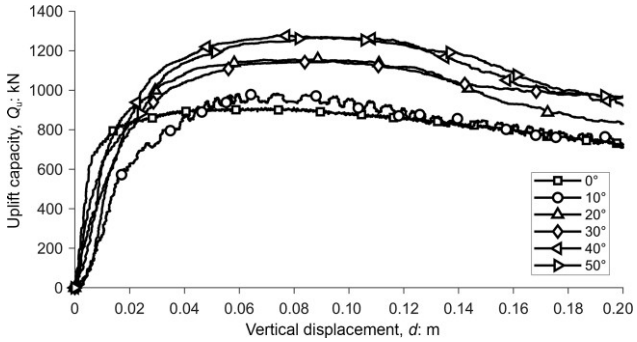

Figure 9. Load–displacement data from centrifuge uplift tests of flat and chamfered pad and column foundation at an embedment ratio of 1 in loose sand ($D_r = 30\%$, 1570 kg/m^3)

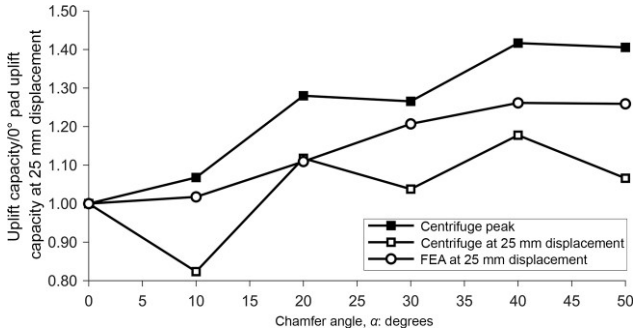

Figure 10. Centrifuge and FEA chamfered pad uplift capacity normalised by capacity of 0° chamfer pad capacity for $H/B = 1$ in medium dense sand ($D_r = 60\%$, 1662 kg/m^3)

Figure 14 appears to show slightly less benefits or a neutral response of increasing backfill density in all cases from FE modelling. This suggests that the majority of the improvements shown in Figure 13 are from the increased mass of the backfill, which was normalised out using the breakout factor. It is notable that the results appear to vary from those of Kulhawy *et al*. (1991), where

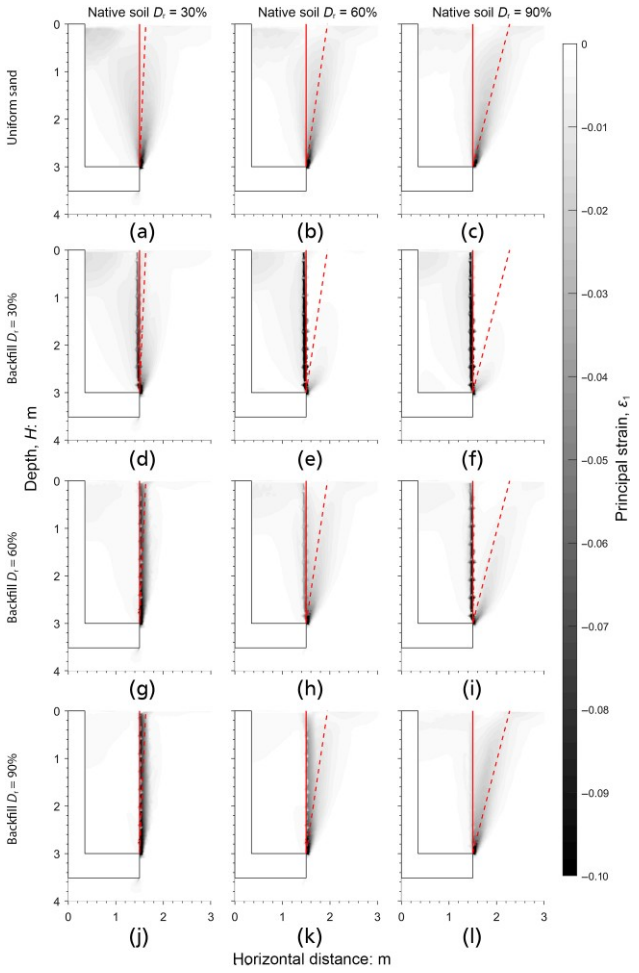

Figure 11. Principal strain after 25 mm uplift showing failure surfaces in different cases for $R_{in} = 1$. Uniform sand (no backfilling or interface elements) at (a) $D_r = 30\%$ (1570 kg/m^3), (b) $D_r = 60\%$ (1662 kg/m^3) and (c) $D_r = 90\%$ (1754 kg/m^3). Backfill with $D_r = 30\%$ and native soil at (d) $D_r = 30\%$, (e) $D_r = 60\%$ and (f) $D_r = 90\%$. Backfill with $D_r = 60\%$ and native soil at (g) $D_r = 30\%$, (h) $D_r = 60\%$ and (i) $D_r = 90\%$. Backfill with $D_r = 90\%$ and native soil at (j) $D_r = 30\%$, (k) $D_r = 60\%$ and (l) $D_r = 90\%$. The solid lines show the vertical and the dashed lines show the dilation angles of the native sand at the given relative density

greater improvement was seen with increasing backfill density. The tests carried out by Kulhawy *et al*. (1991) were undertaken at 1***g*** at about a seventh of the scale of the foundations simulated in the FEA, which in turn would lead to greater soil dilation, a greater tendency to fail outside of the vertical excavation and steeper failure surface inclination angles (especially near the surface). This modelling artefact would increase with greater backfill density where testing was undertaken at vertical in situ stresses less than 10 kPa. Thus, the apparent improvements shown by Kulhawy *et al*. (1991) may have been influenced by the 1***g*** approach to modelling rather than reflecting real full-scale behaviour. This is further highlighted through the comparisons with

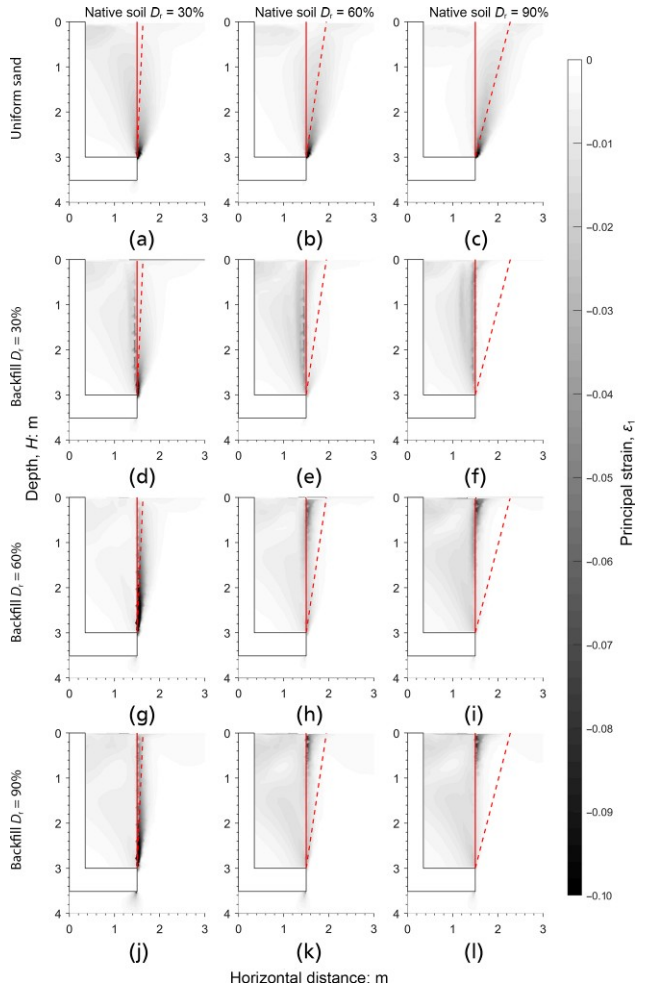

Figure 12. Principal strain after 25 mm uplift showing failure surfaces in uniform sand for R_{in} set to give $\phi_{cs} = 32°$

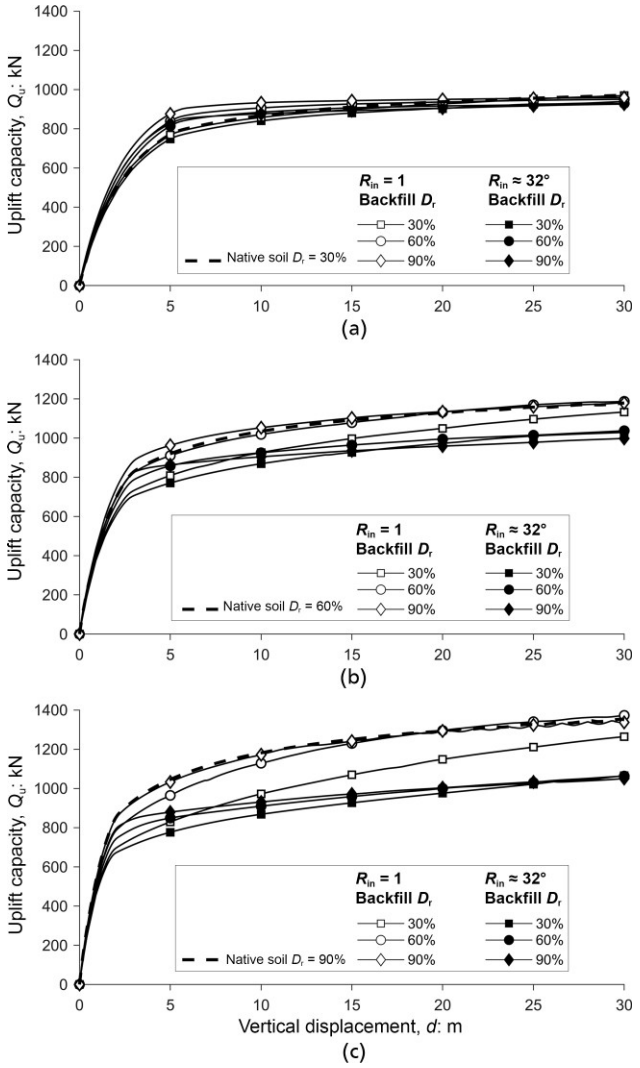

Figure 13. Load–displacement data from uplift of 3 m wide foundation from 3 m depth in native sand with (a) D_r = 30% (1570 kg/m^3), (b) D_r = 60% (1662 kg/m^3) and (c) D_r = 90% (1754 kg/m^3) with backfill of 30%, 60% and 90% relative densities

centrifuge testing (Figure 14), where the stress levels are correct and installation was also simulated and returned a lower capacity than the FE modelling where the foundation was wished in place (i.e. no simulation of installation). It is also notable that Kulhawy *et al*. (1991) placed backfill in a series of lifts that were tamped after supporting casing was raised to the top of each lift. This would result in soil being compacted against the natural soil interface, increasing the initial enhancement. This does not reflect normal UK practice or that adopted in the centrifuge, where the support was raised/removed after complete backfilling to the surface. Although the backfilling approach adopted by Kulhawy *et al*. (1991) differs from the approach here, it may have merit in enhancing the backfill–native soil interface and removing the effects of construction disturbance observed in Figures 12 and 13 and may warrant further investigation.

Although there were differences in the uplift magnitudes between the FE simulations and the centrifuge tests (Figure 14), the results seem consistent with the FEA where a fully disturbed interface was simulated (Figure 15), in that backfilling appears to give less capacity even when the backfill is denser than the native soil (Brown *et al*., 2025). This would suggest that, even if care is taken in physical modelling, any disturbance at the interface on excavation support removal may not be fully captured by FEA (even where a disturbed interface has been simulated). Thus, FEA may be useful to allow mechanism exploration and general trends to be explored, but final predicted uplift magnitudes may require centrifuge or large-scale tests to be undertaken.

For an undisturbed vertical excavation interface, control of the native soil on the global behaviour is made clear in Figure 12(c) where, with a very dense native soil, the effect of backfilling with anything less than this density is a reduced

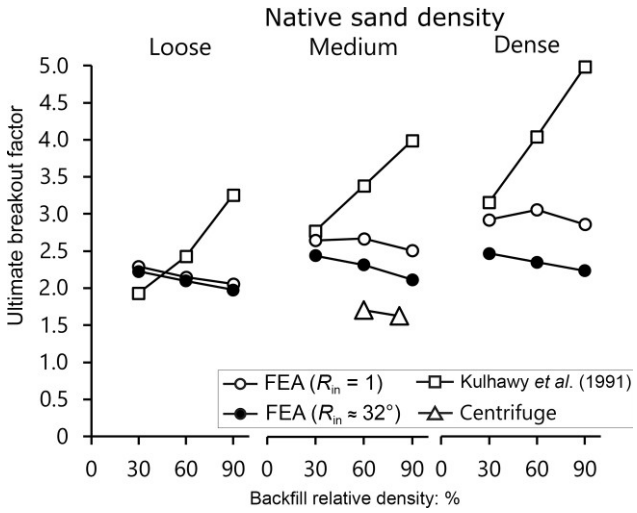

Figure 14. Comparison of uplift breakout factor (N_γ) of capacity at 25 mm for FEA simulations of vertical backfill (Table 3) shown in Figure 13 with data from Kulhawy *et al*. (1991)

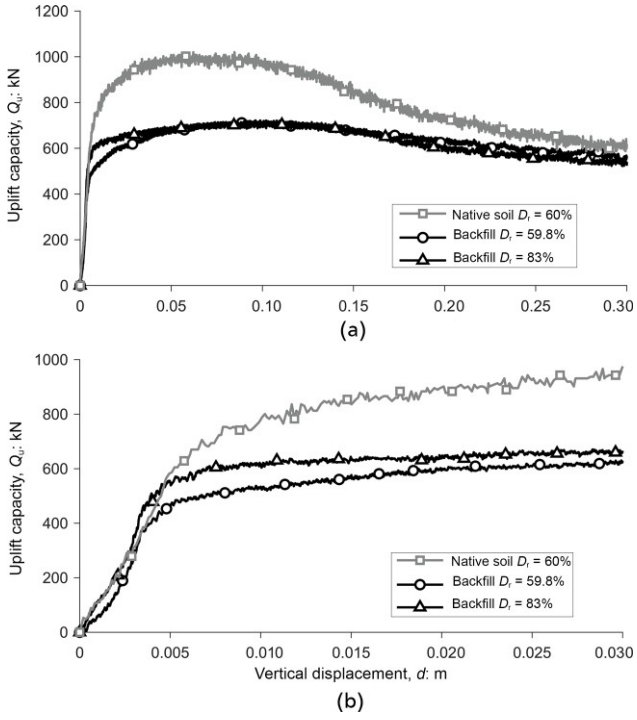

Figure 15. Load–displacement data for pad foundation at $H/B = 1$ in native medium dense sand (1662 kg/m^3) and medium dense backfill (1662 kg/m^3) and dense backfill (1754 kg/m^3) up to (a) 300 mm vertical displacement and (b) 30 mm displacement

capacity for displacements up to 15 mm. This would suggest that, during the construction process, the density of the vertical backfill is carefully controlled and compacted to create as similar a density to the surrounding soil as possible. This is in line with the recommendation 'If backfill is used, its compaction shall be undertaken carefully in order to achieve soil characteristics as close as possible to those of the undisturbed soil' (BSI, 2013a). Achieving this balance in the density of the native and backfill soils will provide greater confidence in the performance of the foundation in uplift, in terms of the available uplift capacity.

When the native sand surrounding the vertical backfilled sand above the foundation was very dense (e.g. $D_r = 90\%$, 1754 kg/m^3), the same behaviour was observed as for the $D_r = 60\%$ scenarios described previously, whereby matching the relative density of the backfill to the native sand gives very similar uplift capacity to the wholly uniform very dense sand condition (Figure 13(c)). Figures 11(c) and 11(i) demonstrate the similarity in the failure surfaces between these two models in terms of the shear strain and development of the failure surface at the dilation angle of the sand. Backfill material constructed with a significantly lower relative density than the surrounding soil will lead to a reduction in uplift capacity and if this is not accounted for during the design phase of the foundation it may be potentially unsafe as the calculated capacity cannot be realised.

Another permutation of the backfill density variations considered was for native soil at a loose relative density ($D_r = 30\%$, 1570 kg/m^3) and backfill at relative densities of 30%, 60% and 90%. In this case there was little variation in the uplift capacity at 25 mm displacement, with the same behaviour observed as before where the matching backfill density led to very similar results to the uniform conditions with no backfill. Increasing the backfill relative density to 60% (1662 kg/m^3) and 90% (1754 kg/m^3) had little effect at the ultimate load, again supporting the suggestion that the native soil density influences behaviour and that compacting to higher levels may be wasted effort. Also, in the case of loose uniform sand, the failure surface was naturally close to the vertical (3.4° for $D_r = 30\%$ (1570 kg/m^3)) due to the low dilation angle and would be naturally similar to any interface created by realistic excavation.

However, the above assumes an undisturbed interface along the vertical excavation surface which, in reality, may be very difficult to achieve without a change in current construction practice in the UK. The results shown in Figures 13–15 suggest that very little gains can be made from additional compaction if the excavation interface is degraded and additional compaction may be wasted effort or result in small gains due the increased weight of the uplifted soil only.

3.3 Excavation inclination

One thing that the FEA study highlighted is that behaviour may be controlled by the native soil, where a vertical excavation can be created without disturbing the excavation interface and the failure surface may pass from the backfilled soil and into the native soil depending on the density and dilation angle. It is also interesting to investigate the limitations of a purely vertical excavation.

Practicality may normally dictate a vertical excavation but if it was shown that inclining the failure surface (Figure 3(b)) would be beneficial, then this could be accommodated in design and construction.

By creating uniform backfill soil conditions in a volume of soil larger than the expected uplift failure wedge, the failure surface would be more likely to form at the dilation angle of the sand instead of following the boundary at the edge of the typically vertical excavations. With careful control over the compaction and the resulting relative density of the backfilled sand, the larger backfilled volume could be useful to improve the foundation uplift capacity in loose sands. As shown earlier (Figure 13(a)), the uplift forces in loose ($D_r = 30\%$, 1570 kg/m^3) native sand with denser backfill in a vertical excavation do not provide any significant gains in capacity. However, if the excavation is sloped beyond the dilation angle of the denser backfilled sand, then the wedge of soil uplifted by the foundation would likely be within the backfill volume and generate uplift forces based solely on the backfill sand properties.

To investigate the effects of inclined sides on the backfill excavation, a 3D FE model was created with the sides of the backfill area sloping at 25° from vertical (Figure 3(b)). Interface elements were included at the boundary between the backfill and native soil areas (varying from $R_{in} = 1$ and R_{in} giving an interface of 32°). A relative density of 30% (1570 kg/m^3) was used for the surrounding soil and the backfill relative density was modelled at 30%, 60% (1662 kg/m^3) and 90% (1754 kg/m^3). Figure 16 shows the principal strain after 25 mm uplift in the three scenarios investigated. In all cases, the failure surface developed at the dilation angle of the backfill sand for the given relative density as per the uniform sand conditions. Figure 16 also includes illustrations of the 25° backfill boundary and the dilation angle of the sand. These simulations were run with the backfill/native boundary interface elements set with $R_{in} = 1$ and with R_{in} required to give ϕ_{cs}, but no variations in the position of the failure surface or uplift capacity were observed as failure occurred within the backfill.

These simulations indicate that inclining the backfill allows the failure surface to develop at the dilation angle, as in uniform soil conditions. However, there appears to be no benefit from inclining the sides of the backfill at an angle greater than the dilation angle of the sand at the respective relative density in terms of mass of soil uplifted. However, if the excavation angle was increased to greater than the dilation angle of the backfill, this would avoid the potential for capacity reductions observed due to failure on a disturbed excavation surface (Figure 13). In any case, any unsupported excavation with inclined sides would need to be at an inclination that exceeds the angle of repose of the native soil for safety reasons.

4. Scope and coverage

The results presented here are valid for rectangular foundations in sand subject to uplift, buried to normalised depths of $H/B = 0.5$–1.5

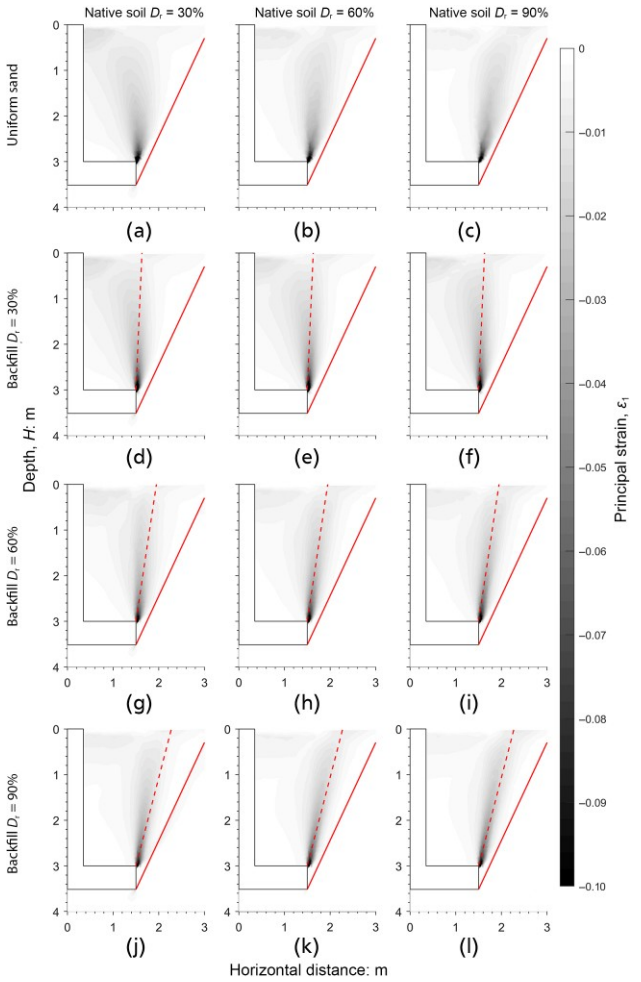

Figure 16. Principal strain after 25 mm uplift showing failure surfaces in different cases for $R_{in} = 1$. Uniform sand at (a) $D_r = 30\%$ (1570 kg/m^3), (b) $D_r = 60\%$ (1662 kg/m^3), (c) $D_r = 90\%$ (1754 kg/m^3). Backfill with $D_r = 30\%$ with 25° sloped backfill and native soil at (d) $D_r = 30\%$, (e) $D_r = 60\%$ and (f) $D_r = 90\%$. Backfill with $D_r = 60\%$ with 25° sloped backfill and native soil at (g) $D_r = 30\%$, (h) $D_r = 60\%$ and (i) $D_r = 90\%$. Backfill with $D_r = 90\%$ with 25° sloped backfill and native soil at (j) $D_r = 30\%$, (k) $D_r = 60\%$ and (l) $D_r = 90\%$. Solid line is at 25° deoting the sloped excavation and the dashed line is dilation angle of the backfill sand at a given relative density

for sands of 30–90% relative density. It is noted that imported granular backfill may be far coarser than sand and thus higher soil friction angles may be generated in this material if it can be adequately compacted. For such material, further investigation would be required. The optimisation of shape was limited to modifying existing construction techniques and foundation geometries. Further optimisation studies could be undertaken from less conventional foundation shapes or by investigating the historical pyramid-shaped foundation as a starting point (Brown *et al*., 2025).

All tests and simulations were undertaken dry or as if the foundation was well above the water table. Future testing could be

undertaken in saturated conditions at various rates in soil with different permeabilities to investigate rate effects and the potential for beneficial suction (Rattley, 2007), although the latter may lead to a non-conservative design case. In addition, only sands were considered in this work and there is further scope for investigation in coarser granular materials and clays (Levy, 2014). The effect of excavation interface disturbance would seem key to backfill behaviour; this has not yet been considered for enhanced shape foundations, which may reduce the gains shown but would still likely result in reduced concrete use. Varying the actual backfill process in vertical excavation systems may have merit based on the results reported by Kulhawy *et al*. (1991), although without further investigation it is difficult to deconvolute what part of their enhancement comes from the small-scale 1***g*** testing methodology or how the foundations were backfilled.

5. Conclusions

Significant investment in OLE is expected in the UK, which will require the construction of new towers and foundations. Typical foundations are concrete pad and column style structures, which require operations and materials that are carbon dioxide intensive. To reduce the environmental impacts and cost of these foundations, studies have been completed to enhance the (design critical) tensile capacity and optimise the foundation shape.

FEA and centrifuge modelling techniques were used to

- investigate the influence of applying a chamfer to the upper edge of the pad foundation on the tensile capacity
- identify the potential benefits of increasing the density of the material used to backfill the excavation around the foundation.

More realistic modelling techniques were used in the centrifuge-based backfill study, which more closely followed field construction methods using formwork to support the excavation during backfill placement, as proposed by Brown *et al*. (2025). The FEA backfill study extended the centrifuge programme to include additional combinations of relative densities and the altered shape of the backfill.

By chamfering the upper edge of the foundation, FEA and centrifuge modelling demonstrated that a gain in tensile capacity of up to 40% at an embedment ratio of 0.5 over the standard square-edged pad foundation is possible. This increase in capacity comes from the transition of the failure surface origin from the top of the pad to the bottom as the chamfer angle was increased from zero to 30–40°. Further increasing the chamfer angle beyond this did not yield greater tensile capacity but would reduce the concrete volume of the pad.

A study of the effect of varying the relative density of the backfill material in relation to the native soil surrounding the foundation and vertical excavation showed that a vertical failure surface formed when the excavation interface was considered undisturbed and the backfill was at a lower relative density than the native soil. When the backfill and native soil relative densities were 60% or greater, in any combination, FEA showed a transitional behaviour with shear planes at the vertical interface and at the dilation angle of the native sand. In the majority of cases there was no significant benefit in increasing the backfill density above that of the native soil, so existing guidance on compacting soils to that of the local surrounding soils would seem sound. However, when the excavation interface was modelled as disturbed, the benefits of backfilling at even the native soil density were less clear. This suggests that how a vertical-sided excavation is constructed and the disturbance induced is key to the potential for backfill enhancement.

Consideration was also given to sloping the backfill excavation sides to 25° to allow the formation of a failure surface at the dilation angle of the sand. The FEA study indicated that the failure surface did form at the dilation angle of the backfill and was not influenced by the excavation. This approach is suggested as a valid technique to increase the uplift capacity when the backfill is compacted to a medium dense or dense state. Sloping the sides beyond the dilation angle of the soil would not provide further benefit in terms of mass of soil uplifted. If the excavation angle was increased to greater than the dilation angle of the backfill, this would avoid the potential for capacity reduction due to failure on a disturbed excavation surface as seen in the vertical excavations. Any unsupported excavation with inclined sides would also need to be at an inclination that exceeds the angle of repose of the native soil for safety reasons.

The results presented in this paper are valid for rectangular foundations in sand subject to uplift buried to normalised depths of $H/B = 0.5$–1.5 for sands of 30–90% relative density.

Acknowledgements

The authors would like to acknowledge the Network Innovation Allowance, without which this project would not have been possible. The authors acknowledge National Grid Electricity Transmission and Scottish and Southern Electricity Networks (SSEN) Transmission for supporting the project and agreeing to publication of the results. The third author is funded by the University of Dundee, the Energy Technology Partnership and SSEN Transmission, and this support is also gratefully acknowledged. The views expressed are those of the authors alone and do not necessarily represent the views of their respective companies or employing organisations.

REFERENCES

Al-Baghdadi TA, Brown MJ and Knappett JA (2016) Development of an inflight centrifuge screw pile installation and loading system. In *Proceedings of the 3rd European Conference on Physical Modelling in Geotechnics (EUROFUGE 2016), Nantes, France*, pp. 239–244.

Al-Defae AHH (2013) *Seismic Performance of Pile-reinforced Slopes*. PhD thesis, University of Dundee, Dundee, UK.

Al-Defae AH, Caucis K and Knappett JA (2013) Aftershocks and the whole-life seismic performance of granular slopes. *Géotechnique* **63(14)**: 1230–1244, 10.1680/geot.12.P.149.

BBC (British Broadcasting Corporation) (2024) *Electricity upgrade plan includes miles of pylons*. BBC, London, UK.

Bentley Systems (2017) *Plaxis 3D Materials Model Manual*. Bentley Systems, Exton, PA, USA.

Bertalot D (2013) *Seismic Behaviour of Shallow Foundations on Layered Liquefiable Soils*. PhD thesis, University of Dundee, Dundee, UK.

Bertalot D, Brennan A and Villalobos F (2013) Influence of bearing pressure on liquefaction-induced settlement of shallow foundations. *Géotechnique* **63(5)**: 391–399, 10.1680/geot.11.P.040.

Brown MJ, Davidson C, Shepherd C, Flint S and Mbisike S (2025) Improved uplift capacity design for overhead line equipment (OLE) in granular soils. *Proceedings of the Institution of Civil Engineers – Geotechnical Engineering* **178**: 793–807, 10.1680/jgeen.25.00006.

BSI (2013a) BS EN 1997-1:2004: Eurocode 7: Geotechnical design – General rules. BSI London, UK.

BSI (2013b) BS EN 50341-1:2012: Overhead electrical lines exceeding AC 1 kV. General requirements – Common specifications. BSI, London, UK.

Cigre (Conseil International des Grands Réseaux Électriques) (2002) *The Design of Transmission Line Support Foundations: An Overview. Report 206. Working Group 22.07 (Foundations)*. Cigre, Paris, France.

Davidson C, Al-Baghdadi TA, Brown MJ *et al.* (2018) Centrifuge modelling of screw piles for offshore wind energy foundations. In *Proceedings of the 9th International Conference on Physical Modelling in Geotechnics (ICPMG 2018), London, UK*, pp. 695–700.

DBEIS (Department for Business, Energy & Industrial Strategy) (2022) *Electricity Networks Strategic Framework: Enabling a Secure, Net Zero Energy System*. DBEIS, London, UK.

Gu KY, Tran NX, Han J *et al.* (2024) Centrifuge study on the uplift behaviour of spread foundation for transmission tower in sand. *Canadian Geotechnical Journal* **61(7)**: 1418–1432.

Kulhawy FH, O'Rourke T, Stewart JP and Beech J (1983) *Transmission Line Structure Foundations for Uplift-Compression Loading, Load Test Summaries: Appendix to EPRI Final Report EL-2870*. Electric Power Research Institute, Palo Alto, CA, USA.

Kulhawy FH, Nicolaides CN and Trautmann CH (1991) Experimental investigation of the uplift behaviour of spread foundation in cohesionless soil. In *EPRI, Report: TR-100220, Project 1493-4*. Electric Power Research Institute, Palo Alto, CA, USA.

Lauder KD (2010) *The Performance of Pipeline Ploughs*. PhD thesis, University of Dundee, Dundee, UK.

Lauder KD, Brown MJ, Bransby MF and Boyes S (2013) The influence of incorporating a forecutter on the performance of offshore pipeline ploughs. *Applied Ocean Research* **39**: 121–130, 10.1016/j.apor.2012.11.001.

Levy F (2014) The Uplift of High Voltage Transmission Tower Foundations. EngD thesis, University of Southampton, Southampton, UK.

Parr RG and Vanner MJ (1962) *Strength Tests on Overhead Line Tower Foundations*. Electrical Research Association, Leatherhead, UK, ERA Report O/T28.

Rattley MJ (2007) The Uplift Behaviour of Shallow Foundations. PhD thesis, University of Southampton, Southampton, UK.

Rattley MJ, Lehane BM, Consoli N and Richards DJ (2008) Uplift of shallow foundations with cement-stabilised backfill. *Proceedings of the Institution of Civil Engineers: Ground Improvement*, **161**: 103–110, 10.1680/grim.2008.161.2.103.

Richards DJ, White DJ and Lehane BM (2010) Centrifuge modelling of the pushover failure of an electricity transmission tower. *Canadian Geotechnical Journal* **47(4)**: 413–424, 10.1139/T09-112.

Shepherd C, Brown MJ, Davidson C, Beckett C and Flint S (2024) Uplift enhancement of steel grillage foundations for overhead line foundations In *Proceedings of XVIII European Conference on Soil Mechanics and Geotechnical Engineering (ECSMGE), Lisbon, Portugal*.

Ueno K (1998) Methods for preparation of sand samples. In *Proceedings of International Conference on Centrifuge*, vol. 2, pp. 1047–1055.

Vanner MJ (2003) Overhead electric power line foundations: past and present practice and future trends. In *Proceedings of the* British *Geotechnical Association International Conference on Foundations*, Dundee, UK, pp. 905–912.

Zmudzinski Z and Sala A (1980) Influence of backfill composition on the loading behaviour of footings. In *Proceedings of International Conference on Compaction, Paris, France*, pp. 207–211.